

Resonant Subband Landau Level Coupling in Symmetric Quantum Well

L.-C. Tung,^{1, a)} X.-G. Wu,² L. N. Pfeiffer,³ K. W. West,³ and Y.-J. Wang^{1, b)}

¹⁾*National High Magnetic Laboratory, Tallahassee, Florida 32310*

²⁾*Department of Physics, Institute of Semiconductor, Chinese Academy of Science, China*

³⁾*Department of Electrical Engineering, Princeton University, Princeton, New Jersey 08544, USA*

(Dated: 23 November 2018)

Subband structure and depolarization shifts in an ultra-high mobility GaAs/Al_{0.24}Ga_{0.76}As quantum well are studied using magneto-infrared spectroscopy via resonant subband Landau level coupling. Resonant couplings between the 1st and up to the 4th subbands are identified by well-separated anti-level-crossing split resonance, while the hy-lying subbands were identified by the cyclotron resonance linewidth broadening in the literature. In addition, a forbidden intersubband transition (1st to 3rd) has been observed. With the precise determination of the subband structure, we find that the depolarization shift can be well described by the semiclassical slab plasma model, and the possible origins for the forbidden transition are discussed.

PACS numbers: 78.20.Ls 78.67.De 73.21.Fg

Keywords: cyclotron resonance spectroscopy, resonant subband Landau level coupling, subband, depolarization, optical nonlinearity

Many terahertz (THz) radiation applications¹⁻³ involve detecting or generating THz radiation using intersubband (ISB) transitions in a quasi-two dimensional electron system (2DES). Designing the 2D heterostructure optimized for desired THz applications demands a comprehensive understanding of the subband structure and ISB couplings. Many intended applications involves optical absorptions in their operations, which can be affected by the depolarization of the radiation. Subband structure and depolarization effect were extensively studied in the past, but the understanding of these subjects are more qualitative than quantitative and sometimes controversial. It is believed that depolarization shifts the absorption energies of the ISB transitions, but the magnitude of the depolarization shift has been calculated using various methods. The depolarization shift can be calculated numerically in the self-consistent calculation by calculating induced changes of the charge densities, but it is not always available and sometimes impossible given the circumstance of the system.

In the past, two of the analytical models have been developed for calculating the depolarization shifts. A semiclassical approach is to calculate the depolarization shift by approximating the 2DES as a slab plasma of thickness d filled with electrons.^{4,5} The depolarization-shifted ISB transition energy $\tilde{\omega}_{10}$ is related to the classical plasma frequency ω_p and ISB transition energy ω_{10} as $\tilde{\omega}_{10}^2 = \omega_{10}^2 + \tilde{\omega}_p^2$, where the effective plasma frequency $\tilde{\omega}_p = (f_{10}\omega_p^2)^{1/2}$ and f_{10} is the oscillator strength of the optical transition. On the other hand, the depolarization shift was described by a microscopic model, in which the overlap of the subband wavefunctions has to be calculated. The shifted ISB transition energy is represented as $\tilde{\omega}_{10} = \omega_{10}\sqrt{1 + \alpha_{10} + \beta_{10}}$,^{6,7} where β_{10} represents the exchange interaction. The depolarization shift is represented by α_{10} and α_{10} is related to the overlap of the subband wavefunction $\phi_i(z)$ via $S_{11} = \int_{-\infty}^{\infty} dz [\int_{-\infty}^z dz' \phi_1(z') \phi_0(z')]^2$. Both of the models have been used to calculate the depolarization shift and agree fairly well with the experimental results. Due to the uncertainty in the function form of the subband wavefunctions in many 2DES systems, it is not yet clear whether the depolarization shift is better described by the microscopic model that considers the wavefunction overlaps, or the semiclassical model that approximates the 2DES as a three dimensional plasma.

To evaluate the magnitude of the depolarization shift, one should first measure the ISB transition energies. ISB transitions have been investigated using optical intersubband-resonance (ISR),^{8,9} magneto-transport measurements^{10,11} and mostly resonant subband Landau level coupling (RSLC). RSLC measures the ISB transition energies by coupling the in-plane cyclotron resonance (CR) orbital motion to the motion along the confinement axes with the presence of a magnetic field parallel to the 2DES. When the CR energy is brought close to the ISB transition energy, CR splits into two modes due to the resonant anti-level crossing of the Landau levels (LLs) belonging to different subbands. It was used to investigate subband structure in heterojunctions,¹²⁻²⁰ parabolic quantum wells,^{21,22} and (asymmetric) quantum wells.(QW)²³⁻²⁵ All of these works focused on the ISB transition between the two lowest subbands and the hy-lying subbands were identified by CR linewidth broadening.^{18,19}

A symmetric QW eases the uncertainties arising from the gradient of the confining potential,⁵ the presence of the depletion charges,¹⁶ and subband's diamagnetic shifts and offsets in k -space.¹⁴ We have selected an ultra-clean, 500Å

^{a)}Electronic mail: tung@magnet.fsu.edu

^{b)}Note: Dr. Wang passed away in Dec. of 2009 due to cardiac arrest.

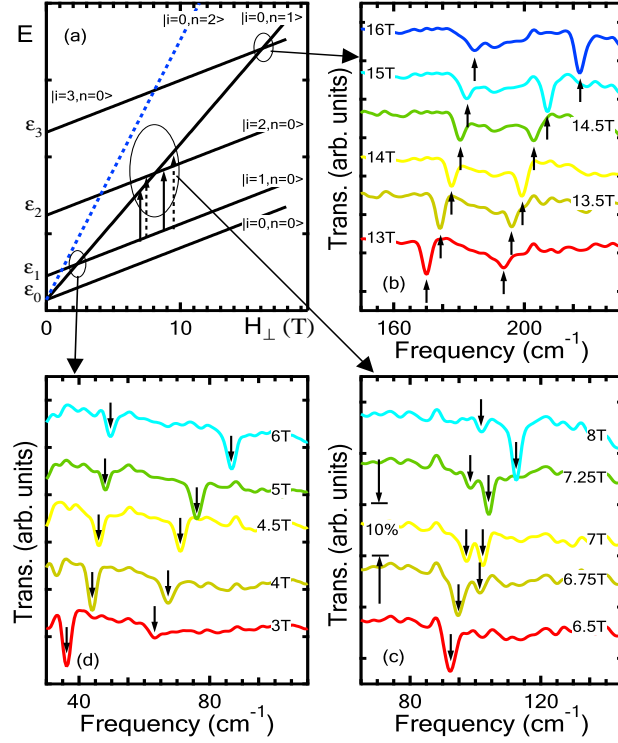


FIG. 1. (a): A schematic energy diagram for the LLs of the subbands. The energies of the LLs are shown as a function of the vertical component of the magnetic field. Each energy level is labeled by the subband index i and LL index n . The anticrossing behavior occurs when the LL transition energy matches the ISB transition energy, i.e. at the crossing points of the $n=1$ LL of the 1st subband and $n=0$ LL of the higher subbands. (the regions enclosed by the circles) Around each anticrossing, split resonance results from the resonant coupling of the LLs belonging to different subbands. The transitions for the lower branch are shown in solid arrows and the ones for the higher branch are shown in dashed arrows. Half-field crossings occur at where the $n=2$ LL of the 1st subband (shown in blue dotted line) crosses the $n=0$ LLs of the higher subbands. One can easily deduce that it will show a bundle of three transitions, and negative magnetic-field dispersion, i.e. the transition energy appears to decrease with increasing magnetic field. (b)-(d): The magneto-infrared spectra for $\theta = 25^\circ$. The traces are shifted vertically for clarity. (b) $B = 13$ to 16 T, for the RSLC between the 1st and 4th subbands. (c) $B = 6.5$ to 8 T, between the 1st and 3rd subbands. (d) $B = 3$ to 6 T, between the 1st and 2nd subbands.

symmetrically doped $\text{Al}_{0.24}\text{Ga}_{0.76}\text{As}/\text{GaAs}/\text{Al}_{0.24}\text{Ga}_{0.76}\text{As}$ QW ($n_s = 1.1 \times 10^{11} \text{cm}^{-2}$) and investigated its subband energies via RSLC by magneto-infrared (IR) spectroscopy at tilt angles from 10° to 35° . In the symmetric QW, the subband wavefunction are better known, and thus the depolarization shift can be estimated more accurately using both of the analytical models. We find that the depolarization shift can be better described by the semiclassical slab plasma model and have observed a resonant coupling forbidden in the first order perturbation.

A set of magneto-IR spectra ($\theta = 25^\circ$) are displayed in Fig. 1 (b)-(d) and a schematic energy diagram is displayed in Fig. 1 (a). It is plotted in scale using the subband energies obtained from the self-consistent calculation, which excludes the depolarization shift. Since the 2DES enters the extreme quantum limit at around 2.2 T, only the $n=0$ and $n=1$ LLs of the first subband need to be considered. At the resonance of the LL and ISB transitions, i.e. when the CR energy matches the ISB transition energy, split resonances result from the anti-level crossing between the $n=1$ LL of the first subband and the $n=0$ LLs of the higher subbands. With increasing magnetic field, the lower-energy mode transfers its integrated intensity to the higher-energy mode, as shown in Fig. 1 (b)-(d). RSLC to the hy-lying subbands are observed by the well-separated split resonance and the energies of the split resonance can be precisely extracted to study the ISB transitions to the hy-lying subbands.

The energies of the split resonance as a function of the magnetic fields at five different angles are plotted in Fig. 2. The dotted lines show the expected CR energies that scale with $\cos\theta$. We will refer the anticrossings as the first, second and third, ordered by their energies in ascending order. The energies of the split resonance around the first anticrossing can be well described by the coupled oscillator model^{26,27} with $m^* = 0.069m_e$, and $\tilde{\omega}_{10} = 57 \text{cm}^{-1}$.

To get a picture of the transitions particularly for those resulting from the resonant coupling to the hy-lying subbands, coupled Schrödinger and Poisson equations are solved self-consistently in order to obtain the subband

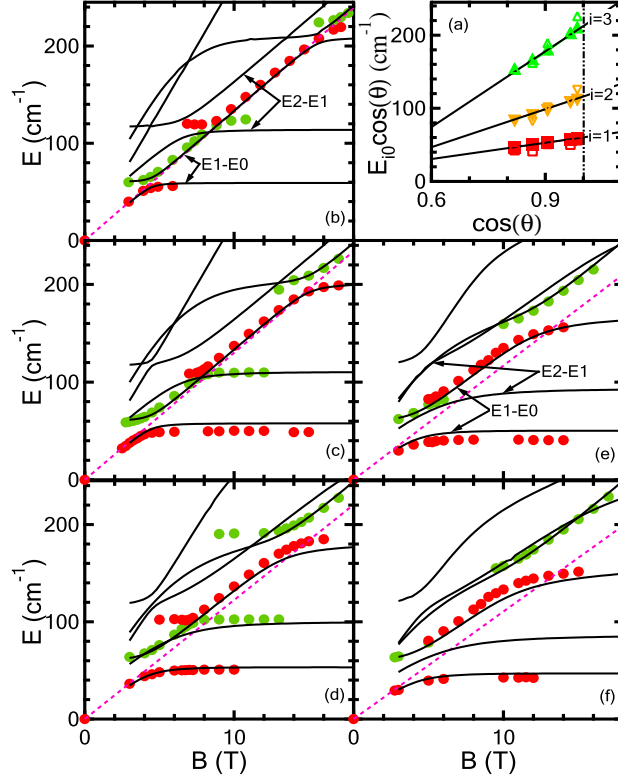


FIG. 2. The energies of the split resonance as a function of magnetic field for different angles: (b) 10° , (c) 15° , (d) 25° , (e) 30° and (f) 35° . The solid lines are results of the self-consistent calculation including the depolarization shift. The dotted lines represent the expected CR energies that scale with $\cos\theta$. (a): Pinning energies of the lower branches of the anticrossings are plotted against $\cos\theta$. The pinning energies extracted from the measurements are shown in open symbols, while the ones extracted from the self-consistent calculation are shown in solid symbols.

energy levels in the presence and absence of the magnetic field.⁵ The 2DES is confined in a 500 \AA QW with finite barrier. The barrier height is determined from the Al fraction in the barrier material. We have selected the lower one (180 meV) of the two band offsets used in the literature. Since the QW is wide, the lowest subband energy is insensitive to the selection of the barrier height, while the higher subbands are slightly affected. The conduction-valence bandgap is around 1520 meV and the magnetic field range in this work is not too high, so the conduction band non-parabolicity is ignored. Without using any perturbation, the subband energies and the matrix element for the depolarization are calculated by an exact diagonalization of the Hamiltonian, which includes the LL subband coupling.

Using the linear-response approximation, depolarization shifts are taken into account by considering the induced oscillating electron density along the direction of the confinement, when the frequency-dependent dynamic conductivity is evaluated.⁵ The electron density along the well direction is assumed to be symmetric about the center of the QW. The formulation is similar to, but not exactly the same as ref. [5]. Our calculation stops at just calculating the resonance frequencies, whereas the oscillator strength were also calculated in the literature.

In the numerical calculation, material parameters are taken for GaAs, and typically 25 subbands with 8 or 16 LLs are included in the self consistent calculation. In considering the depolarization shift, the lowest 20 energy levels are taken into account. The excitonic shift is ignored, since its effect is negligible in a wide quantum well.^{5,21} The result of the self-consistent calculation is shown in solid lines in Fig. 2, and the calculated transition energies agree well with the measured transition energies when the depolarization shift are considered.

To determine the magnitude of the depolarization shift, we will have to extract the ISB transition energies from the experimental results and compared them with the ones calculated by excluding the depolarization shift. Instead of using the mid-points between the split resonance,¹⁶ we extract the ISB transition energies using the pinning energies of the lower branches of each anticrossing. The lower branches of each anticrossing pin at around $\tilde{\omega}_{i0} \cos\theta$ at high fields as shown in Fig. 2 (a). The pinning energies decrease linearly with decreasing $\cos\theta$ for measured and calculated transition energies. It is surprising that the linear dependence still holds even when the sample is tilted 35° . The ISB transition energies can then be extracted by extrapolating the pinning energy to $\cos\theta \sim 1$ (i.e. $\theta = 0$) and the results

	Exp. (cm^{-1})	Theo. (depol.)	ex. depol.
$\tilde{\omega}_{10}$	57	60	31
$\tilde{\omega}_{20}$	116	116	110
$\tilde{\omega}_{30}$	216	212	218

TABLE I. Measured subband energies: One column lists the experimental values for the anticrossings, while the other list the theoretical values when the depolarization effect is included (depol.) or excluded (ex. depol.).

are listed in Table 1.

By comparing the ISB transition energies in Table 1, the energy of the first anticrossing is nearly doubled due to the depolarization shift, leaving others unaltered. Unlike the previous works, we are dealing with a much simpler system, which leaves narrow margins to fine tune the result. In the past, studies over the depolarization shifts were carried out mostly on heterojunctions, in which the gradient of the confining potential and the presence of the depletion charges were usually unknown, leading to uncertainties in the wavefunction forms and thus the magnitude of the depolarization shift. In this wide and symmetric QW, subband wavefunctions will be close to the ones in the infinite quantum well of the same width. Using the subband wavefunctions of an infinitely deep QW, the depolarization shift for the 1st anticrossing can be represented as $\tilde{\omega}_{10}^2 = \omega_{10}^2 + \frac{5}{3}\omega_p^2$. Using sample's parameters, the depolarization shifted ISB transition energy is then $69cm^{-1}$, but it is much larger than the measured values. One should note that this discrepancy cannot be overcome by tuning the energy spacings between the subbands using different material parameters. The measured ISB transition energy is simply smaller than $\sqrt{\frac{5}{3}}\omega_p$, leaving no space for fine tuning. A finite QW is expected to have an even larger depolarization shift, since it has been demonstrated by Fishman⁷ that S_{11} calculated using wavefunctions for a finite QW is larger than the ones using wavefunctions for an infinite QW. The depolarization shift for the two hy-lying subbands are negligible, since the energy spacings are much larger than the plasma frequency ω_p and the leading factors are small.⁷

Alternatively and more simply, depolarization shifts were calculated using the slab plasma model.^{4,5} Using the oscillator strength for an infinite QW,²¹ $f_{10} \sim 0.96$, the depolarization-shifted ISB transition energy $\tilde{\omega}_{10}$ is $56cm^{-1}$, consistent with the result of this work. For the 2nd and 3rd anticrossings, depolarization shifts are minimal, since $f_{30} \sim 0.03$ and $f_{20} \sim 0$ (forbidden). It appears that the results are better described by the semiclassical model. The proof of this claim can be pursued by finding the carrier concentration dependence of the depolarization-shifted ISB transition energies.

The ISB transition between the 1st and 3rd subband is forbidden due to symmetry, but a resonant coupling between the CR and the forbidden ISB transition has been observed. With increasing tilt angles, the lower branch of the anticrossing (E2-E1) between the 3rd and 2nd subbands is depressed below the upper branch of the one (E1-E0) between the 2nd and the 1st subbands, thus the 2nd anticrossing becomes more difficult to resolve with increasing tilt angle. It is not a half-field crossing of the third anticrossing, since those should be associated with a negative magnetic-field dispersion and appears as a bundle of three transitions.¹⁵ Moreover, half-field crossings require the QW to be asymmetric in order to have a significant energy separation between the split resonance,²⁹ and sufficient population in the $n = 1$ LL of the first subband to yield sufficient intensity for the half-field-crossing split resonance. Introducing a modest linear potential along z -axes increases the intensity of this symmetry-forbidden split resonance, but it also significantly reduces the energy of the third anticrossing.

Exceptions of the selection rules for optical transitions in 2DES have been reported recently in InSb²⁵ and InAs²⁸ quantum wells, which were explained in terms of the multiband $\mathbf{k}\cdot\mathbf{p}$ perturbation theory. In the one band model (conduction band only), a transition from the 1st to the 3rd subband is not allowed; however, if the influence of the valence band is considered, the selection rules may be relaxed,²⁵ though it will be very weak, since the conduction-valence bandgap is rather large in GaAs.

Another possibilities is that the ISB transition may still be forbidden, but a resonant coupling to the forbidden transition becomes possible when the higher-order couplings are considered. Neglected higher-order terms in the theoretical calculation²⁹ may be responsible for this symmetry-forbidden anticrossing. It has been suggested that QWs may have large third-order optical nonlinearity^{30,31} when the photon energy matches the ISB transition energy. Some nonlinearity contributions³¹ depend on a relaxation time, which measures the time needed for the system to relax from the non-equilibrium state to the equilibrium state. In this ultra-clean system, it is likely to take longer time for the electron subsystem to relax, since the scattering rate should be much lower due to high mobility.

In summary, we have investigated the subband structures and the ISB transitions via RSLC in an ultra-clean symmetric QW. For the first time, RSLC to the hy-lying subbands are observed by well-separated split resonance, including a symmetry-forbidden resonant coupling. We find that the depolarization shifts can be better described by the slab plasma model.

ACKNOWLEDGMENTS

We like to thank P. Cadden-Zimansky and Jinbo Qi for their assistance. The measurements were performed at NHMFL at Tallahassee, supported by National Science Foundation and the state of Florida.

- ¹B. Ferguson and X. C. Zhang, *Nature Mater.* **1**, 26 (2002)
- ²P. H. Siegel, *IEEE Trans. Microwave Theory Tech.* **50**, 910 (2002)
- ³X. G. Guo, Z. Y. Tan, J. C. Cao and H. C. Liu, *Appl. Phys. Lett.* **94**, 201101 (2009)
- ⁴W. P. Chen, Y. J. Chen and E. Burstein, *Surf. Sci.* **58**, 263 (1976)
- ⁵T. Ando, A. B. Fowler and F. Stern, *Rev. Mod. Phys.* **54**, 437 (1982)
- ⁶T. Ando, *Z. Phys. B* **26**, 263 (1977)
- ⁷G. Fishman, *Phys. Rev. B* **27**, 7611 (1983)
- ⁸A. D. Wieck, K. Bollweg, U. Merkt, G. Weimann, and W. Schlapp, *Phys. Rev. B* **38**, 10158 (1988)
- ⁹J. Y. Anderson and G. Landgren, *J. Appl. Phys.* **64**, 4123 (1988)
- ¹⁰K. Ensslin, C. Pistitsch, A. Wixforth, M. Sundaram, P. F. Hopkins and A. C. Gossard, *Phys. Rev. B* **45**, 11407 (1992)
- ¹¹K. Ensslin, A. Wixforth, M. Sundaram, P. F. Hopkins, J. H. English and A. C. Gossard, *Phys. Rev. B* **47**, 1366 (1993)
- ¹²Z. Schlesinger, J. C. M. Hwang and S. J. Allen Jr, *Phys. Rev. Lett.* **50**, 2098 (1983)
- ¹³G. L. J. A. Rikken, H. Sigg, C. J. G. M. Langerak, H. W. Myron, J. A. A. J. Perenboom, and G. Weimann, *Phys. Rev. B* **34**, 5590 (1986)
- ¹⁴M. A. Brummel, M. A. Hopkins, R. J. Nicholas, J. C. Portal, K. Y. Cheng, and A. Y. Cho, *J. Phys. C: Solid State Phys.* **19**, L107 (1986)
- ¹⁵A. D. Wieck, J. C. Maan, U. Merkt, J. P. Kotthaus, K. Ploog, and G. Weimann, *Phys. Rev. B* **35**, 4145 (1987)
- ¹⁶K. Ensslin, D. Heitmann and K. Ploog, *Phys. Rev. B* **39**, 10879 (1989)
- ¹⁷J. Pillath, E. Batke, G. Weimann, and W. Schlapp, *Phys. Rev. B* **40**, 5879 (1989)
- ¹⁸J. G. Michels, R. J. Nicholas, G. M. Summers, D. M. Symons, C. T. Foxon, and J. J. Harris, *Phys. Rev. B* **52**, 2688 (1995)
- ¹⁹Z. Chen, C. M. Hu, P. L. Liu, G. L. Shi and S. C. Shen, *J. Appl. Phys.* **82**, 3900 (1997)
- ²⁰Y. Sugimoto, S. Takaoka, K. Oto, T. Saku, and Y. Hirayama, *Solid State Commun.* **127**, 629 (2003)
- ²¹K. Karrai, H. D. Drew, M. W. Lee, and M. Shayegan, *Phys. Rev. B* **39**, 1426 (1989)
- ²²L. Brey, N. F. Johnson and B. I. Halperin, *Phys. Rev. B* **40**, 10647 (1989)
- ²³M. B. Stanaway, C. J. G. M. Langerak, R. A. J. Thomeer, J. M. Chamberlain, J. Singleton, M. Henini, O. H. Hughes, A. J. Page, and G. Hill, *Semicond. Sci. Technol.* **6**, 208 (1991)
- ²⁴R. Winkler, *Surf. Sci.* **361/362**, 411 (1996)
- ²⁵J. M. S. Orr, K.-C. Chuang, R. J. Nicholas, L. Buckle, M. T. Emeny and P. D. Buckle, *Phys. Rev. B* **79**, 235302 (2009)
- ²⁶R. Borroff, R. Merlin, R. L. Greene, and J. Comas, *Superlattices and Microstructures* **3**, 493 (1987)
- ²⁷M. Merlin, *Solid State Commun.* **64**, 99 (1987)
- ²⁸R. J. Warburton, C. Gauer, A. Wixforth, J. P. Kotthaus, B. Brar and H. K. Kroemer, *Phys. Rev. B* **53**, 7903 (1996)
- ²⁹M. Załuzny, *Phys. Rev. B* **40**, 8495 (1989)
- ³⁰M. Załuzny, *Appl. Phys. Lett. Rev.* **61**, 2509 (1992)
- ³¹S. Y. Yuen, *Appl. Phys. Lett.* **43**, 813 (1983)